J. Min. Metall. Sect. B-Metall. 61 (1) (2025) 27 - 41

Journal of Mining and Metallurgy, Section B: Metallurgy

HYDROTHERMAL LEACHING BEHAVIOR OF A COMPLEX POLYMETALLIC SECONDARY SULFIDE CONCENTRATE ENHANCED BY ULTRASONICATION

Q.F. Liu, Y.L. Liao*, J.L. Li, M. Wu

Faculty of Metallurgical and Energy Engineering, Kunming University of Science and Technology, Kunming, China

(Received 18 June 2024; accepted 21 March 2025)

Abstract

Complex polymetallic secondary sulfide concentrate (CPSSC) is difficult to be efficiently utilized because of its special mineral phase structure and high lead and iron content. A novel process proposed in this study, hydrothermal leaching without acid (water as lixiviate) enhanced by ultrasonic, can achieve environmentally friendly and selective separation of copper from CPSSC and prevent the production of the hazardous material plumboferrite contained in the leached residue. The influence of the control parameters on the leaching efficiency and the mineral phase composition and structure of the obtained leached residue is investigated. The obtained results show that the leaching efficiency of copper without sulfuric acid, is the best under the conditions of temperature 180 ℃, oxygen partial pressure 1.0 MPa, stirring speed 600 r/min, ultrasonic power 360 W, liquid to-solid ratio 10:1 and mass ratio of lignosulfonate to raw material 0.2%. Under the above optimal conditions, the leaching efficiency of copper and iron reached 99.12% and 19.46%, respectively. Ultrasonic amplification increases the leaching efficiency of copper by 10.02%, and promotes the leaching efficiency of iron, which decreases by 5.20%. The leaching process conforms to the model of unreacted contraction core model under mixed control, the activation energy is 71.76 kJ/mol, and the macroscopic kinetic equation in terms of stirring rate, oxygen partial pressure and ultrasonic power is $1-(1-X)^{1/3}-1/3\ln(1-X) = 40.457P_{O2}^{0.071}r^{0.903}e^{(-8630.19/T)}t$.

Keywords: *Chalcopyrite; Process enhancement; Hydrothermal leaching; Kinetics*

1. Introduction

Chalcopyrite ($CuFeS_2$) is the most common and most widespread copper bearing mineral. However, with the continuous mining of copper ores, not only has the copper content of the original chalcopyrite ore decreased year by year, but it is also it present together with iron, lead, arsenic and other elements. Moreover, the flotation properties of copper and lead are similar, so it is still difficult to obtain the concentrates required for the pyrometallurgical process from the original chalcopyrite ore through beneficiation. This resulted in the existence of a large number of complex polymetallic secondary sulfide concentrates (CPSSC). When the CPSSC is treated using the traditional pyrometallurgical method, the copper recovery is low, and the process produces, a large amount of lead scum and hazardous gases. Although lead scum contains some copper and lead, it is difficult to be recycled. The produced harmful gases, such as CO, N_xO_y, and SO_2, pose a potential threat to the environment and the human body. In comparison, hydrometallurgy is more economical and environmentally friendly to extract valuable metals like copper from CPSSC. Hydrometallurgical leaching of CPSSC shows great potential in terms of addressing the environmental impacts and lowering treatment costs [1]. However, due to the unique mineral phase structure of chalcopyrite the main mineral phase existing in CPSSC [2], passivating layers which consist of bimetallic sulfides, polysulfides, elemental sulfur and jarosite can be formed on the surface of the chalcopyrite particles during leaching, resulting in low leaching efficiency of the valuable metals [3, 4]. This limits the promotion and development of this environmentally friendly method for the disposal of CPSSC. Therefore, it is urgent to strengthen the leaching process of CPSSC and improve the leaching efficiency of copper to utilize this kind of resource.

In recent years, methods to enhance chalcopyrite leaching include pretreatment activation and strengthening during leaching process have been researched and reported. Pretreatment activation includes mechanical activation [5-7], thermal activation [8] and microwave activation [9, 10], which can improve the reactivity of chalcopyrite in leaching.

Corresponding author: liaoyl@kust.edu.cn

https://doi.org/10.2298/JMMB240618003L

The strengthening methodology in the leaching process includes adding additives such as pyrite [11, 12], Ag ions [13, 14] and activated carbon to strengthen the leaching [15, 16], and external field strengthening by ultrasonic field, microwave field [17, 18] and pressure field [19].

However, the leaching strengthened by the pressure field was able achieve more than 98% leaching efficiency of Cu from low-grade polymetallic complex chalcopyrite ore. The conditions required for the leaching process are harsh with a high temperature (200 °C) and high O_2 partial pressure (1.2 MPa) [20]. Therefore, it is necessary to study pressure enhanced leaching under gentle conditions. Studies have shown that the leaching efficiency of copper from chalcopyrite is significantly improved when the leaching system is in the ultrasonic field [21-24]. Wang's investigation demonstrated that the leaching efficiency of copper increased to 57.5% from 50.4% in an oxygenated acidic ferric solution while ultrasonic enhancement was performed in leaching process of concentrated chalcopyrite containing 18.2% Cu [25]. Yoon [26] used $FeCl_3$ solution as lixiviant to dispose chalcopyrite ($CuFeS_2$) containing 41.5% Cu, and under the enhanced action of ultrasound, the leaching efficiency of copper increased to 87% from 77%. When the ultrasonic field was induced in the leaching system, an ultrasonic cavitation effect was generated, resulting in high temperature, high pressure, and luminous discharge phenomena in some micro-areas in the leaching solution. By creating such an extreme environment, ultrasound could improve the efficiency of material transfer and phase interface renewal, and promote the break of intermolecular bonding bonds to activate the molecules, thus playing a significant role in promoting the leaching process [27]. The research conducted by Wang [28] showed that the leaching efficiency of copper increased to 6.2% from 5.4% while the leaching process of low grade of primary copper sulfide ore containing 0.49% Cu was enhanced with ultrasonic in comparison to that of without enhancement. However, the leaching systems involved in these studies are mainly high-valent iron ion systems with strong oxidation, or in strongly acidic medium. The medium without acid for hydrothermal leaching and the kinetics of the leaching methodology enhanced with ultrasonic were rarely involved, especially not in oxygen pressurized system. Moreover, the raw materials used in these studies were concentrated chalcopyrite or primary sulfide copper ore, but not in refractory ore such as CPSSC, and even with concentrated chalcopyrite the obtained leaching efficiency of copper was not ideal.

From the above studies, it can be seen that both pressure field and ultrasonic strengthening can improve the leaching efficiency of copper from chalcopyrite, but there are few studies on the combination of ultrasonic and pressure field to strengthen leaching of copper from CPPSC. In this paper, a novel process for eco-friendly utilization of CPSSC by the joint application of pressure field and ultrasonic filed was proposed. The effects of reaction temperature, initial acidity, oxygen partial pressure, stirring speed, ultrasonic power and liquid solid ratio on the leaching of CPSSC were studied, and the kinetics of ultrasonically enhanced copper leaching without acid (water as leaching agent) from CPSSC was studied.

2. Experimental

2.1. Materials and chemical agents

In the present work, CPSSC produced in beneficiation operations was kindly supplied by a concentrator of a mining company in Yunnan Province, China. First, it was crushed with a ball mill (XMQ240×90, Jiangxi Victor International mining equipment Co., LTD, China) and screened with a standard Taylor sieve, so that raw materials with a particle size of -45 μm were obtained for the experiment. The content of chemical elements in the raw materials was determined by inductively coupled plasma emission spectrometry (ICP-AES) while the samples were dissolved with a mixture of hydrochloric, nitric and perchloric acids. The specific results are presented in Table 1 which shows that besides the copper content of the raw material is only 11.10%, far below the copper concentrate content required (Cu >18%) for disposing by traditional pyrometallurgical methodology, while the content of iron and lead is high. Obviously, the raw material used in the present work was a typical low-grade polymetallic complex copper sulfide secondary concentrate.

X-ray diffractometer (XRD, X 'Pert Pro MPD) was used to analyze the mineral phase composition of the raw material, and the obtained results were shown in Figure 1. Fig. 1 shows that the mineral phases contained in CPSSC include chalcopyrite ($CuFeS_2$), bornite (Cu_5FeS_4), pyrite (FeS_2), galena (PbS), sphalerite (ZnS) and quartz (SiO_2).

Table 1. *Chemical elemental analysis of raw materials*

Cu	Fe	Pb	Zn	S	SiO_2	CaO	Al_2O_3	MgO	Others (CO_3^{2-}, SiO_3^{2-})
11.1	28.1	8.88	2.97	34.95	8.86	1.68	0.5	1.63	1.33

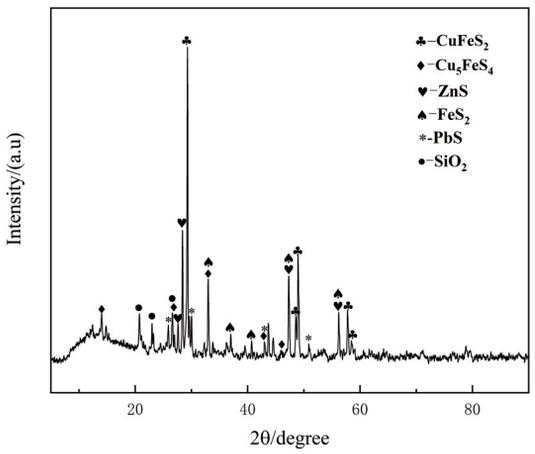

Figure 1. *XRD pattern of raw material*

2.2. Instruments and experimental method

The effects of reaction temperature, initial acidity, oxygen partial pressure, stirring speed, ultrasonic power and the ratio of liquid to solid on the leaching efficiency of copper and iron and the concentration of sulfuric acid in the reaction system for hydrothermal leaching enhanced by ultrasonic were studied. First, 30 g of the raw material with a particle size of -45 μm and the specified volume of water or diluted sulfuric acid according to a specified ratio of liquid to solid were added into the autoclave equipped with ultrasonic irradiation (YZUR-500M, Shanghai Yancheng Instrument Co., LTD.). The mixture was then heated to the required temperature under continuous agitation, and oxygen was continuously introduced through a vent value from the oxygen cylinder to maintain a constant pressure and simultaneously ultrasonic with a specified power was induced to react for 4 h. During the leaching process, the concentration of copper, iron and sulfuric acid in the leaching solution was analyzed by sampling at an interval of 15 min for the first two hours and of 30 min for the last two hours. Finally, the autoclave was cooled in the air to a temperature below 50 ℃ and venting out the gas in the autoclave after the experiment was completed, and the obtained pulp was removed and filtered with a vacuum filter apparatus to get the leachate and the leached residue. The leached residue was dried in an oven at 105 ℃ for 2 h before further analysis. Samples were taken from the obtained leachate was sampled to test the content of copper, zinc, iron and sulfuric acid.

2.3. Analysis and characterization methods

The mineral phases and morphology of the raw material and the leached residue obtained were characterized by XRD and scanning electron microscopy (SEM, Hitachi Regulus8100). After the raw material and the leached residue were pretreated by dissolving with acid, the chemical composition of the raw material and the leached residue was quantitatively analyzed by inductively coupled plasma emission spectrometry (ICP-AES, Optima-5300DV). The content of copper, iron and free sulfuric acid in the solution was determined by iodimetry, tin (II) reduction-potassium dichromate titration and acid-base neutralization titration, respectively.

The leaching efficiency of copper and iron was calculated according to formula (1).

$$\eta_x = \frac{w_{xi}}{w_{x0}} \times 100\% \quad (1)$$

Where: η_x is the leaching efficiency of copper, zinc and iron; w_{xi} is the mass of copper and iron contained in the leaching solution, and w_{x0} is the mass of copper and iron contained in the raw material.

In addition, during the study of copper leaching kinetics, the leaching efficiency of copper at different times was calculated according to equation (2).

$$X_i = \frac{\left(V_0 - \sum_{i=1}^{i-1} V_i\right) \cdot C_i + \sum_{i=1}^{i-1} V_i \cdot C_i}{W_{xo}} \quad (2)$$

Where: X_i is the copper leaching efficiency at the i time of sampling;

V_0 is the total volume of leached liquid before sampling;

V_i is the volume of the i sample;

C_i is the concentration of copper in the leaching solution at the i time of sampling;

W_{xo} is the mass of copper in the raw material.

3. Results and Discussion

3.1. Leaching mechanism without acid

3.1.1. Thermodynamically feasible and spontaneous of leaching reactions

In order to determine the thermodynamic feasibility and spontaneity of the chemical reaction for the leaching of valuable metals from CPSSC, it is necessary to calculate the probability of its progress (delta G). Under the conditions for the leaching of valuable metals from CPSSC, the main chemical reactions and their standard Gibbs energy were listed in Table 2.

From the value of the standard Gibbs energy in Table 2, it suggests that the chemical reactions of the realized leaching are thermodynamically feasible and spontaneous as the reason that the standard Gibbs

Table 2. *Standard Gibbs energy (kJ/mol) of the main chemical reactions in leaching*

Chemical reaction	$\Delta_rG^\theta_{298K}$	$\Delta_rG^\theta_{393K}$	$\Delta_rG^\theta_{413K}$	$\Delta_rG^\theta_{433K}$	$\Delta_rG^\theta_{453K}$
$2FeS_2 + 7O_2 + 2H_2O = 2Fe_2^+ + 4H^+ + 4SO_4^{2-}$	-559.887	-513.637	-503.686	-490.798	-477.203
$4FeS_2 + 15O_2 + 2H_2O = 4Fe^{3+} + 4H^+ + 8SO_4^{2-}$	-1162.16	-1052.2	-1029.56	-999.058	-965.251
$FeCuS_2 + 4H^+ + O_2 = Cu^{2+} + Fe^{2+} + 2S^0 + 2H_2O$	-80.899	-63.64	-60.737	-59.304	-56.571
$2ZnS + 4H^+ + O_2 = 2Zn^{2+} + 2S_0 + 2H_2O$	-87.935	-84.557	-82.276	-80.952	-78.443
$2FeS_2 + 4H^+ + O_2 = 2Fe^{2+} + 4S^0 + 2H_2O$	-74.513	-67.331	-64.842	-62.97	-60.989
$2PbS + 4H^+ + 2SO_4^{2-} + O_2 = 2PbSO_4 + 2S^0 + 2H_2O$	-99.773	-103.375	-104.714	-105.528	-106.557
$S^0 + 2H_2O + 3O_2 = 4H^+ + 2SO_4^{2-}$	-288.792	-226.165	-222.128	-216.792	-211.23

energy (ΔrG_T^θ) of these reactions during leaching is minus. Although it is known that chalcopyrite is dissolve in an acidic leaching medium, water can be used as a leaching agent in the present work. This is because the FeS_2 contained in the CPSSC reacts with water and oxygen to produce sulfuric acid, which is needed to dissolve chalcopyrite, and during the leaching process, sulfuric acid could be produced from the oxidation of S^0.

Although sphalerite and galena were contained in CPSSC besides chalcopyrite, in the experimental study under the leaching conditions controlled in this study, galena and sphalerite were found to react and dissolve easily. Galena was transformed into lead sulfate or lead alum remained in the leached residue, and the zinc contained in the sphalerite was leached into the leachate in the form of zinc sulfate. Additionally, comparing the value of the standard Gibbs energy used to dissolve ZnS, PbS and $FeCuS_2$ in Table 2, it can be seen that $FeCuS_2$ is more difficult to leach than ZnS and PbS. This is because the delta G of the leaching reaction of $FeCuS_2$ is the largest.

3.1.2. Effect of initial concentration of sulfuric acid

Under the conditions of a reaction temperature of 180 °C, an oxygen partial pressure of 0.6 MPa, stirring speed of 500 r/min, an ultrasonic power of 360 W, a liquid-solid ratio of 10 mL /g, a reaction time of 4 h and a mass ratio of lignosulfonate to raw material of 0.2%, the change of copper leaching efficiency with leaching time under different initial sulfuric acid concentrations (without sulfuric acid, acid concentration 5 g/L, 10 g/L, 15 g/L and 20 g/L) were shown in Figure 2.

Figure 2 shows that chalcopyrite can be dissolved by maintaining a high sulfuric acid concentration at the initial reaction, and that the copper leaching efficiency gradually increases with the increase of initial acidity. When the initial concentration of sulfuric acid was 0 g/L (no sulfuric acid was added, but water was used as lixiviate), the copper leaching efficiency was low in the first 30 min duration, mainly because the leaching reaction of chalcopyrite must involve hydrogen ions, and the increase of acidity was conducive to copper leaching. With the direct oxidation of pyrite (FeS_2) to produce sulfuric acid (see the reaction expressed as equation (3)), the acidity of the reaction system continues to increase, and the leaching system can provide sufficient acid for the leaching of copper in chalcopyrite.

$$4FeS_2 + 15O_2 + 2H_2O = 4Fe^{3+} + 8SO_4^{2-} + 4H^+ \qquad (3)$$

It can be demonstrated that the leaching of copper from CPSSC containing pyrite (FeS_2) can be achieved by using water as lixiviate under the conditions of oxygen pressurized atmospheric system.

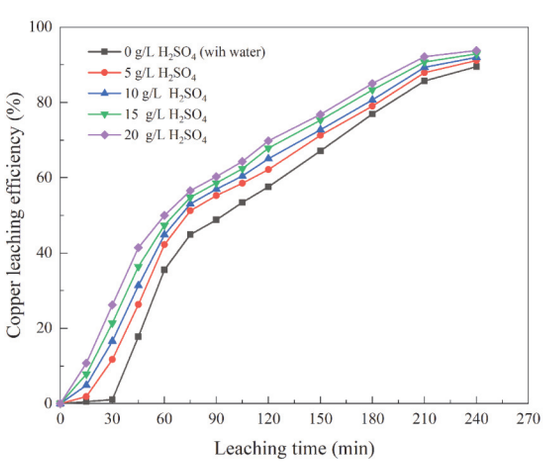

Figure 2. *Influence of initial acidity on copper leaching efficiency*

3.2. Effects of leaching parameters

3.2.1. Effect of leaching temperature

Under the conditions of water as lixiviate, oxygen partial pressure 0.6 MPa, stirring speed 500 r/min, ultrasonic power 360 W, liquid-solid ratio 10 mL/g, reaction time 4 h, and mass ratio of lignosulfonate to raw material 0.2%, The influence of different leaching temperatures (120 °C, 140 °C, 160 °C, 180 °C and 190 °C) on the leaching efficiency of copper, zinc and

iron, as well as the concentration of iron and sulfuric acid in the leaching solution with the leaching time was studied, and the obtained results are shown in Figure 3.

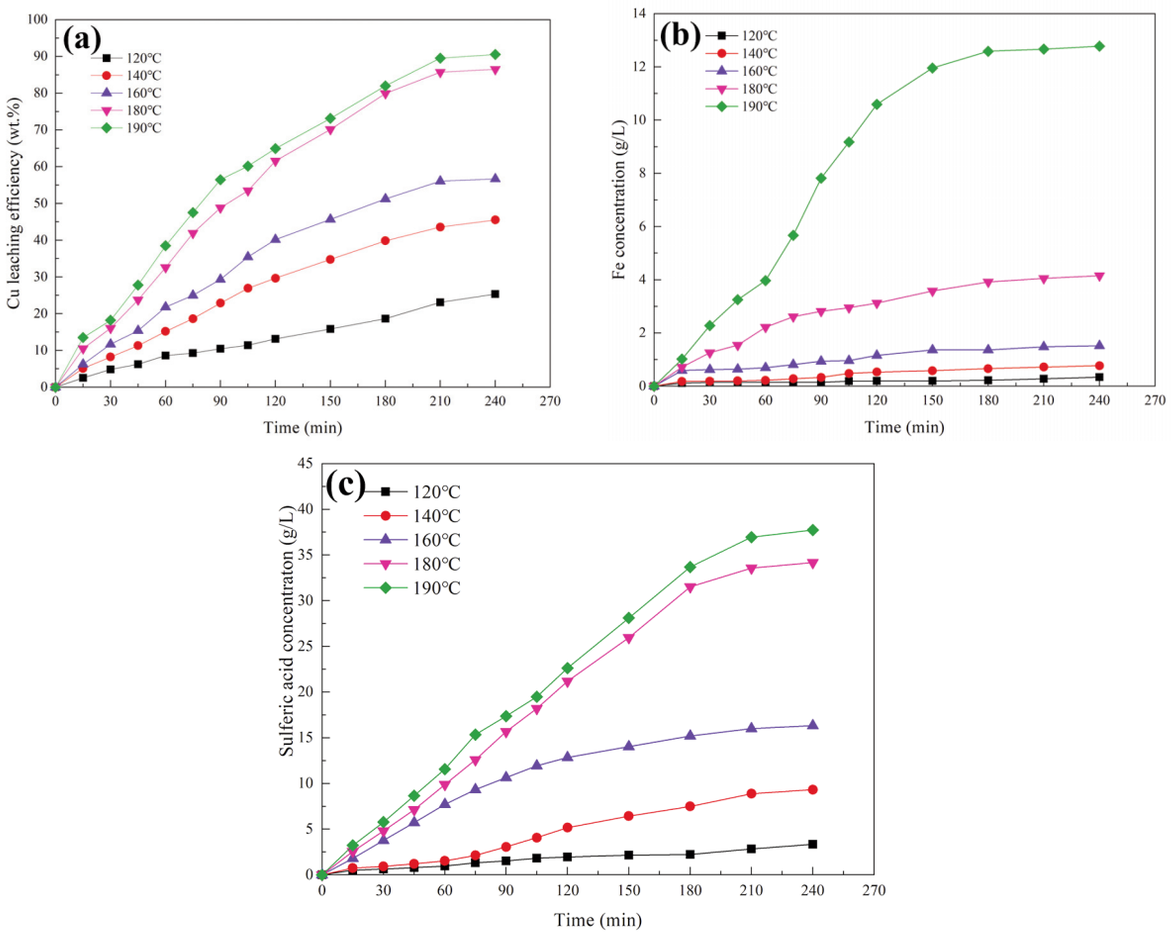

Figure 3. *Influence of temperature on leaching process: (a) copper leaching efficiency, (b) iron concentration, and (c) sulfuric acid concentration index leaching for 4 h*

Figure 3 shows that the leaching efficiency of copper, zinc, and iron, as well as the concentration of iron and sulfuric acid in the leachate increased with the increase in reaction temperature. Under the condition of reaction temperature 120 °C, pyrite (FeS_2) directly reacts with oxygen and water to produce sulfuric acid at a slow rate, for this reaction is insufficiently completed and the residual amount of hydrogen ions generated to react with chalcopyrite, galena, and sphalerite is small, resulting in a low concentration of sulfuric acid in the reaction system and low leaching efficiency of copper and zinc. With the increase of reaction temperature, the oxidation dissolution of pyrite (FeS_2), which can produce sulfuric acid, becomes sufficient, the leaching efficiency of copper, zinc and iron increases resulting from the dissolution of chalcopyrite becoming sufficient, and the final concentration of sulfuric acid in the leachate also increases. Figure 2(d) also shows that the leaching of zinc from CPSSC is easier than that of copper during leaching at the conditions involved in the present work. Only when a good leaching efficiency of copper is achieved, the leaching of zinc from CPSSC can be realized. Therefore, the leaching behavior of valuable metals from CPSSC should focus on the leaching of copper.

XRD analysis of the leached residue (see Figure 4) shows that unreacted chalcopyrite, pyrite and sphalerite are present in the leached residue obtained at 120 °C, and the diffraction peaks of the above three substances have become less obvious at 160 °C, while only plumboferrite, ferric oxide and lead sulfate phases are detected in the leached residue obtained at 180 °C.

The leached residues at different reaction temperatures were analyzed by SEM/EDS, and the

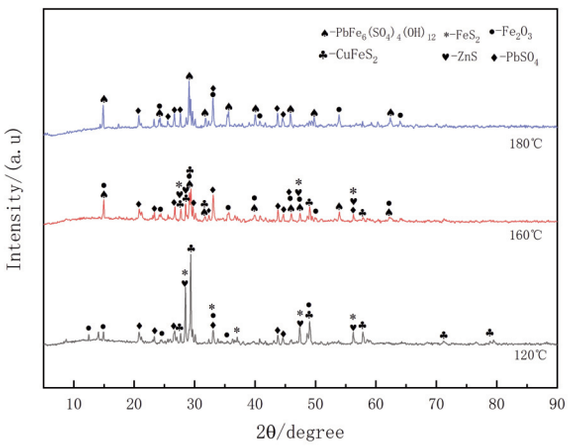

Figure 4. *XRD patterns of leached residue at different temperatures*

obtained results are shown in Figure 5 and Figure 6. In Figure 5 it can be seen that Cu is present in the leached residue when leached at 160 °C, and combined with the XRD data (Figure 4), it can be demonstrated that the leaching reaction is incomplete, and the surface of the leached residue obtained is coated with the reaction products plumboferrite and hematite. As shown in Figure 6, the leaching reaction was completed at 180 °C, and the main components of the leached residue obtained were hematite, lead sulfate and a small amount of plumboferrite. These experimental results showed that increasing the reaction temperature was beneficial to the leaching reaction, leading to the mineral phases in the leached residue obtained mainly existed into hematite and lead sulfate.

3.2.2. *Effect of oxygen partial pressure*

Under the conditions of a reaction temperature of 180 °C, water as lixiviate, a stirring speed 500 r/min, an ultrasonic power of 360 W, a liquid-solid ratio of 10 mL/g, a reaction time of 4 h and a mass ratio of sodium lignosulfonate to raw material of 0.2%, the effects of different oxygen partial pressures (0.4, 0.6, 0.8, 1.0 and 1.2 MPa) on the copper leaching efficiency were shown in Figure 7.

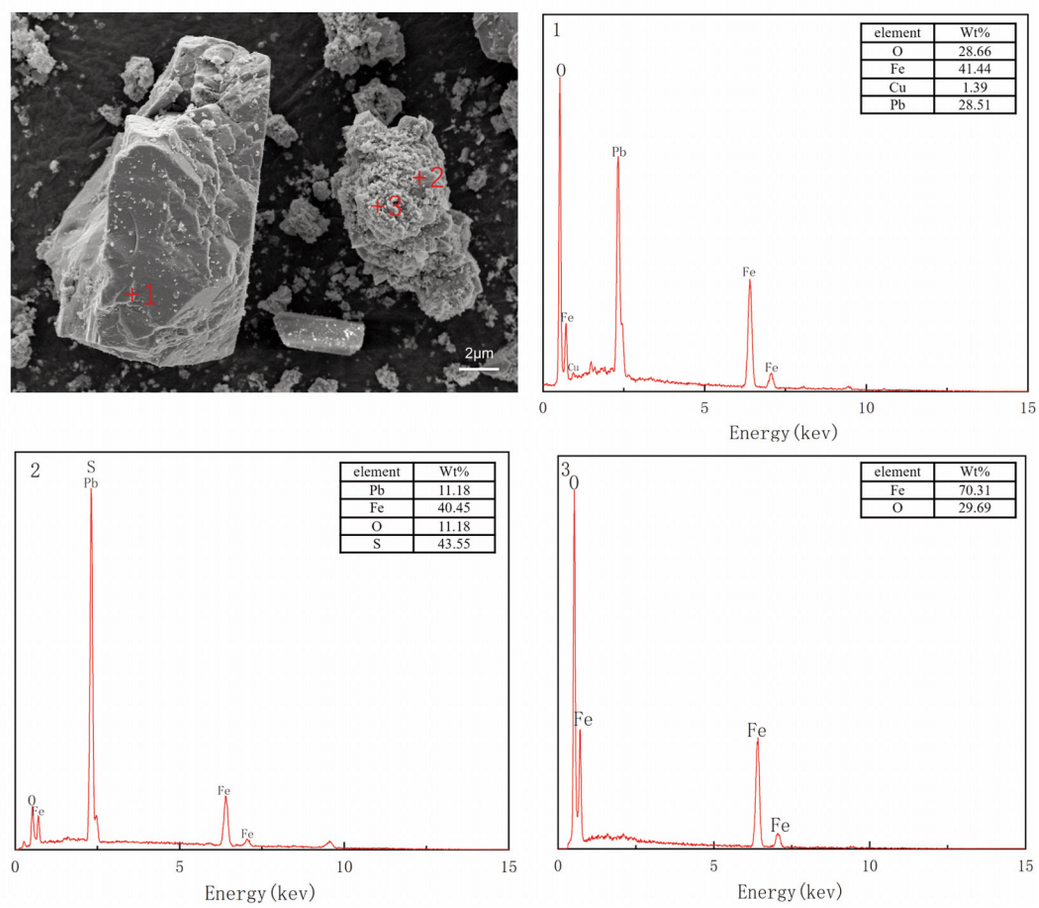

Figure 5. *SEM-EDS spectra of leached residue at 160 °C*

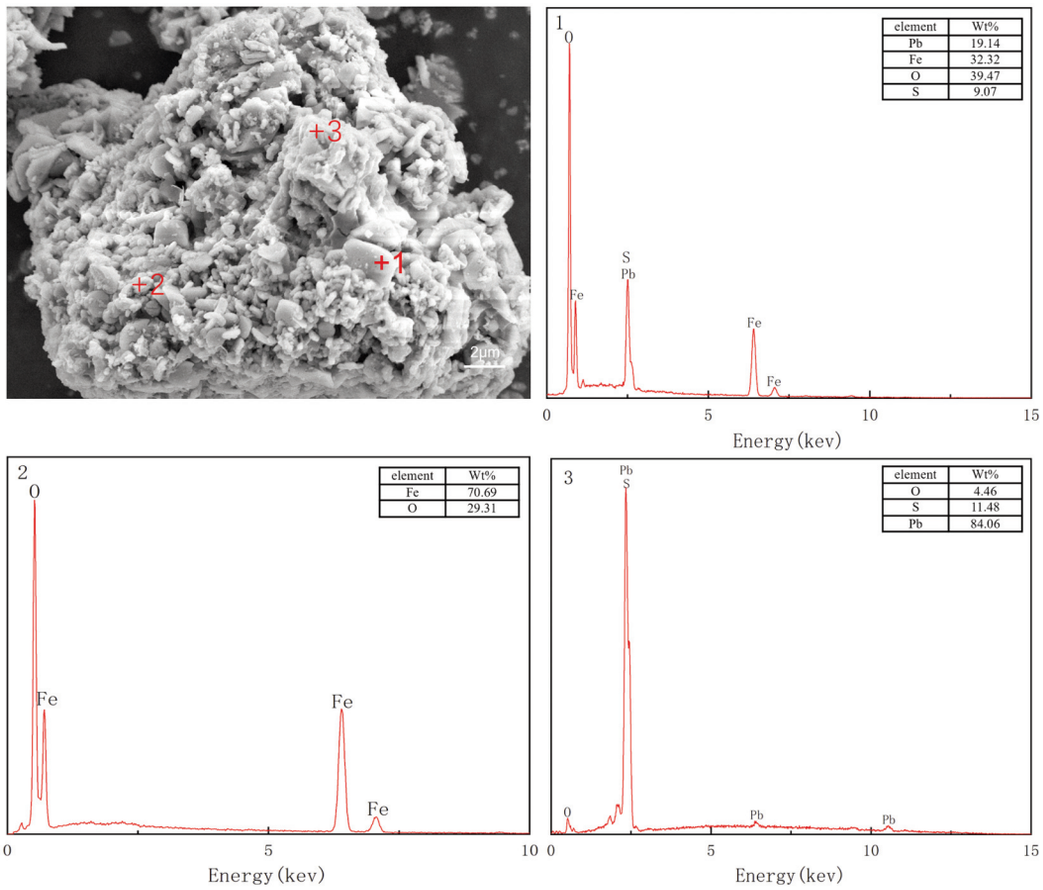

Figure 6. *SEM-EDS spectra of leached residue at 180 ℃*

Figure 7 shows that the leaching efficiency of copper increases with increasing oxygen partial pressure in the range of 0.4-1.2 MPa. But the growth rate of copper leaching efficiency in the range of 0.4-1.0 MPa is larger than that of during the rage between 1.0-1.2 MPa. This is mainly because increasing the partial pressure of oxygen is conducive to increasing the dissolved oxygen in the leaching solution, thus accelerating the oxidation and dissolution of minerals such as pyrite (FeS_2) and chalcopyrite in the raw materials. However, when the oxygen partial pressure increases to a certain extent, the concentration of dissolved oxygen in the leaching solution gradually reaches saturation, so the influence of copper leaching efficiency on the increase of oxygen partial pressure is not significant. The high oxygen partial pressure leads to the conversion of sulfur in the sulfide into sulfuric acid, and the acidity in the solution increases, limiting the hydrolysis of iron ions and increasing the leaching efficiency of iron in the solution. It was also found that the iron content in the leaching solution increased with the increase of iron leaching efficiency in the range of 1.0-1.2 MPa oxygen partial pressure. However, the high oxygen partial pressure places higher requirements for the manufacturing of the equipment used for leaching, increasing the investment if this process is further applied in the future. The optimal oxygen partial pressure is determined as 1.0 MPa.

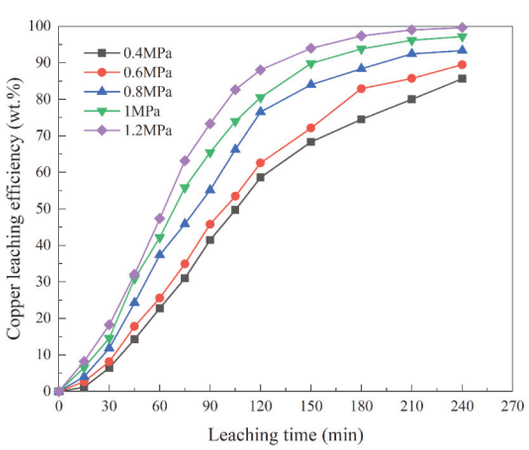

Figure 7. *Influence of oxygen partial pressure on copper leaching efficiency*

3.2.3. Effect of stirring speed

Under the conditions of reaction temperature 180 °C, water as lixiviate, oxygen partial pressure 1.0 MPa, ultrasonic power 360 W, liquid-solid ratio 10 mL/g, reaction time 4 h and mass ratio of sodium lignosulfonate to raw material 0.2%, the effects of different stirring speeds (300, 400, 500, 600 and 700 r/min) on copper leaching efficiency were shown in Figure 8.

As shown in Figure 8, in the stirring speed range of 300 r/min to 600 r/min, the copper leaching efficiency increases with the stirring speed. There are two reasons accounting for this phenomenon. One is that by enhancing the agitation speed the distribution of minerals in the leaching solution can become more uniform and the contact between the reactants can become more adequate. The other reason is that the high stirring speed can improve the diffusion of oxygen and hydrogen ions. When the stirring speed exceeds 600 r/min, the concentration of hydrogen ions and oxygen concentrations on the surface of chalcopyrite has gradually reached saturation, so strengthening the diffusion of oxygen and hydrogen ions can no longer improve the oxidation reaction of chalcopyrite.

Moreover, the leaching efficiency of copper does not increase significantly in the stirring speed range of 600 r/min to 700 r/min. It can be found that increased agitation can promote not only the oxidation reaction of chalcopyrite, but also the dissociation of pyrite and the oxidation reaction of sulfur during the leaching process, resulting in a continuous increase in the acidity of the leaching solution, a decrease in the hydrolysis rate of iron ions, and finally a continuous increase in the leaching rate of iron ions. The optimal stirring speed is chosen as 600 r/min.

3.2.4. Effect of ultrasonic power

Under the conditions of reaction temperature 180 °C, water as lixiviate, oxygen partial pressure 1.0 MPa, stirring speed 600 r/min, liquid-solid ratio 10 mL/g, reaction time 4 h and mass ratio of sodium lignosulfonate to raw material 0.2%, the effects of without ultrasound and with different ultrasonic power (90, 180, 270, 360 and 450 W) on the copper leaching efficiency and the morphology of the leached residue were shown in Figure 9 and Figure 10, respectively.

Figure 9 shows that the copper leaching efficiency increases with the increase of the ultrasonic power when the ultrasonic power is below 360 W. And Figure 10 shows that the particles of the obtained leached residue are small and porous and covered with reaction products on their surface the higher the ultrasonic power is, indicating that the leaching reaction is more adequate. In addition, the particle distribution analysis of the leached residue enhanced by ultrasonic with power of 0 W, 180 W and 360 W was analyzed using a laser particle size analyzer (Malvern Mastersizer 3000, Great Britain). The obtained data of Dv (90) were 16.636, 12.902 and 11.136 μm respectively. The reason for the above phenomenon is that the cavitation effect of the ultrasonic wave and the extreme environment of high temperature and high pressure are generated in the micro-area, which catalyzes the strengthening of the chemical reaction and improves the leaching efficiency of copper [29, 30]. In addition, it can be seen from the experimental results in Figure 8 that the copper leaching efficiency no longer increases significantly with the increase of ultrasonic power when the ultrasonic power exceeds 360 W. This phenomenon is due to the fact that with the further

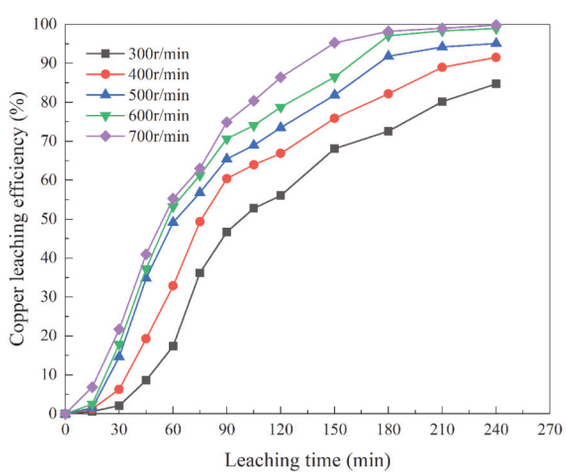

Figure 8. *Influence of stirring speed on copper leaching efficiency*

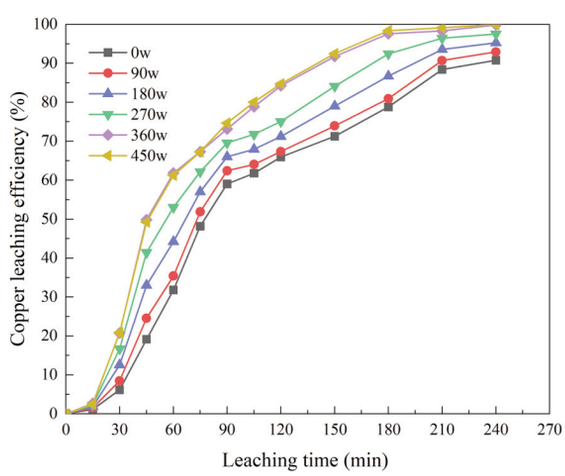

Figure 9. *Influence of ultrasonic power on copper leaching efficiency*

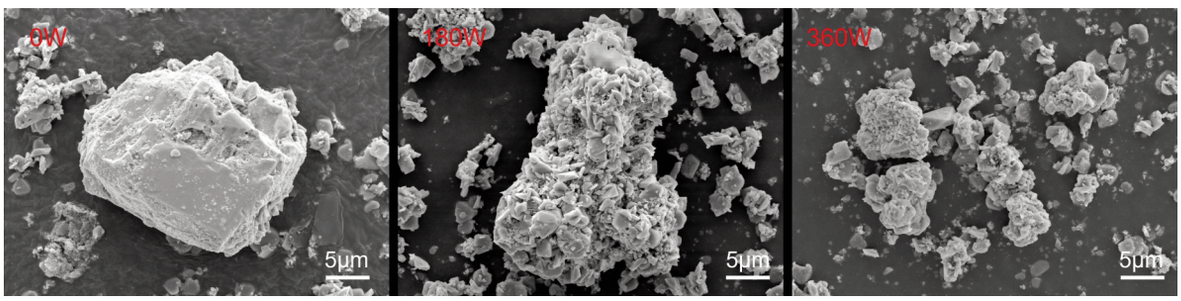

Figure 10. *SEM images of leached residue under different ultrasonic power*

increase of ultrasonic power, too concentrated holes are formed near the ultrasonic generation probe, which affect the conduction of sonic waves, weaken the strengthening effect, and ultimately lead to the reduction of reaction efficiency [31, 32]. The optimal ultrasonic power was set at 360 W.

3.2.5. Leaching behavior under optimal conditions

The raw material was added into the autoclave equipped with ultrasonic irradiation for hydrothermal leaching enhanced by ultrasonic under the optimal conditions determined as above. At a reaction temperature of 180 ℃, water as lixiviate, an oxygen partial pressure of 1.0 MPa, a stirring speed of 600 r/min, a liquid-solid ratio was 10 mL/g, and a mass ratio of sodium lignosulfonate to raw material of 0.2%, the reaction was irradiated for 4 h with an ultrasonic power of 360 W. The average results of three parallel experiments showed that the leaching efficiency of copper and iron were 99.12% and 19.64%, respectively. Moreover, the leaching efficiency of copper with ultrasonic irradiation was 10.02% higher than that of without ultrasonic irradiation, and the leaching efficiency of iron with ultrasonic irradiation was 5.20% lower than that of without ultrasonic irradiation.

3.3. Copper leaching kinetic analysis

3.3.1. Choice and determination of the kinetic model

For the kinetic analysis of the leaching process, it is necessary to select a kinetic model. According to the preliminary analysis, the leaching process of the CPSSC belongs to the gas-liquid-solid multiphase reactions. The analysis of the chemical reaction occurring in the leaching process, shows that solid phase products such as hematite, sulfur elemental and plumboferrite are generated during the reaction process, which are easily coated on the surface of the unreacted chalcopyrite. Therefore, the kinetic analysis of the hydrothermal leaching process under oxygen pressure enhanced by an ultrasonic field was carried out using the unreacted core shrinkage model [33, 34]. According to the theory of the model, there are three kinds of chemical reaction speed control steps, which are chemical reaction control, internal diffusion control and mixed control which are jointly determined by two factors. The specific rate equations were listed as equation (4), (5) and (6).

$$1-\left(1-X\right)^{1/3}=K_r t \tag{4}$$

$$1-2/3X-\left(1-X\right)^{2/3}=K_d t \tag{5}$$

$$1-\left(1-X\right)^{1/3}-1/3ln\left(1-X\right)=K_m t \tag{6}$$

Where X is the copper leaching efficiency, t is the reaction time; K_r, K_d and K_m are the apparent rate constants of chemical reaction control, internal diffusion control and mixing control, respectively.

The data in Figure 3(a) were substituted into equations (4), (5) and (6) for linear fitting, and the results obtained are shown in Figure 11. Figure 11 shows that the correlation coefficients of chemical reaction control and mixing control fitting are close to 1, indicating that the hydrothermal leaching process under oxygen pressure of CPSSC enhanced in the ultrasonic field conforms to both chemical reaction control and mixing control models.

The reaction rate constants of chemical reaction control and mixing control fitted at different temperatures were substituted into the Arrhenius equation to obtain the apparent activation energy. The Arrhenius equation was given in equation (7).

$$K=Ae^{(-E/RT)} \tag{7}$$

Where A is the frequency factor, E is the apparent activation energy (kJ/mol), R is the gas equilibrium constant (8.314 J/mol), and T is the thermodynamic temperature (K).

Equation (8) could be obtained by taking logarithm of both sides of equation (7):

$$lnK = -E / RT + lnA \quad (8)$$

lnK was used to plot versus 1/T (figure 12) and linear fitting was performed. The apparent activation energy (E) of the chemical reaction control and mixing control was 39.36 kJ/mol and 71.76 kJ/mol, respectively, and the frequency factor A was 71.02 and 1.039×10^5, respectively. Since the activation energy controlled by the chemical reaction was greater than 41.8 kJ/mol [35-38], it was further indicated that hydrothermal leaching of CPSSC enhanced by ultrasonic under oxygen pressure belongs to mixing control model, and its kinetic

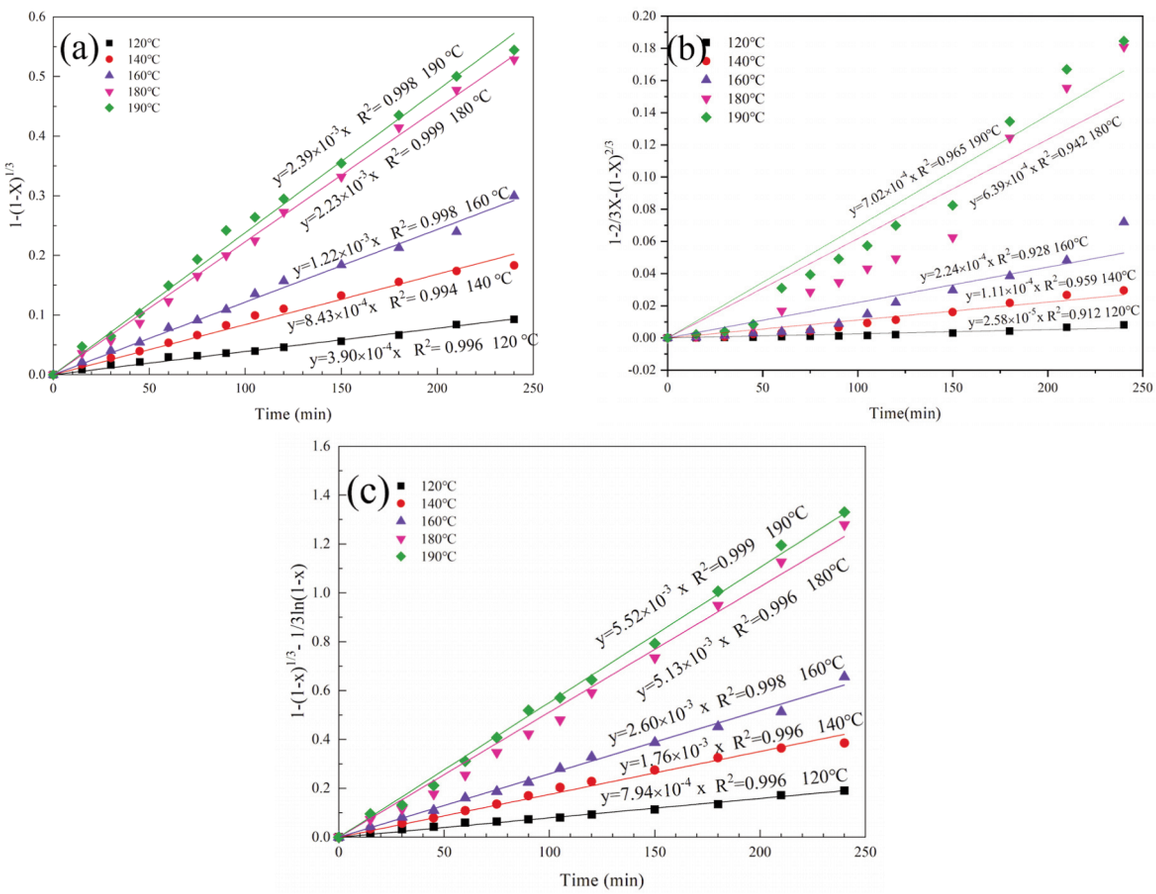

Figure 11. *Fitting results of control model: (a) chemical reaction control, (b) internal diffusion control and (c) mixing control*

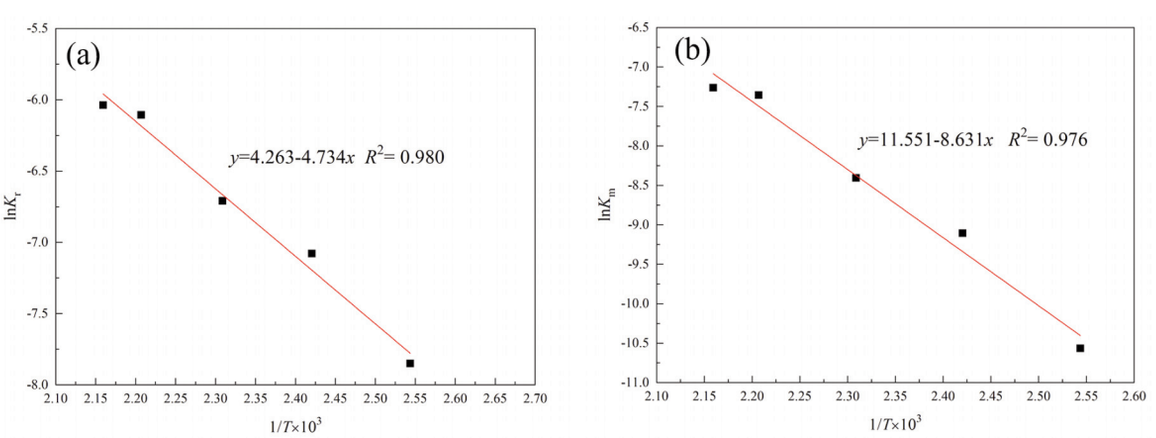

Figure 12. *Relationship between lnK and 1/T at different control model: (a) chemical reaction control, (b) mixing control*

equation could be expressed as equation (9).

$$1-(1-X)^{1/3}-1/3ln(1-X)=1.039\times10^{5}e^{[-71760/(RT)]}t \quad (9)$$

3.3.2. Kinetics equation deduction

On the basis of determining the kinetic equation of the leaching reaction, the effects of ultrasonic power, oxygen partial pressure and stirring speed on the leaching process were quantitatively analyzed. The relationship between copper leaching efficiency and the time in the mixed control process could be expressed by the macroscopic dynamic equation of equation (10) [39].

$$1-(1-X)^{1/3}-1/3ln(1-X)=k'P_{O_2}^{n_1}r^{n_2}P^{n_3}e^{[-E/(RT)]}t \quad (10)$$

where P is ultrasonic power (W), P_{O2} is the partial pressure of oxygen (MPa), r is stirring speed (r/min), k′ is the temperature dependent constant, and n_1, n_2, n_3 are the reaction order of ultrasonic power, oxygen partial pressure and stirring speed, respectively.

3.3.2.1. Reaction order of oxygen partial pressure

Leaching data related to oxygen partial pressure (Figure 7) were brought into the dynamic equation of hybrid control for linear fitting, and the fitting results were shown in Figure 13(a). The natural logarithm ($\ln K_m$) of constant velocity K_m obtained in the range of 0.4-1.2 MPa was plotted against the natural logarithm ($\ln P_{O2}$) of oxygen partial pressure (Figure13(b)), and linear fitting was carried out, resulting in the reaction order (n_1) of oxygen partial pressure was obtained as 0.771.

3.3.2.2. Reaction order of stirring speed

Leaching data related to stirring speed (Figure 8) were brought into the dynamic equation of mixing control for linear fitting, and the fitting results were

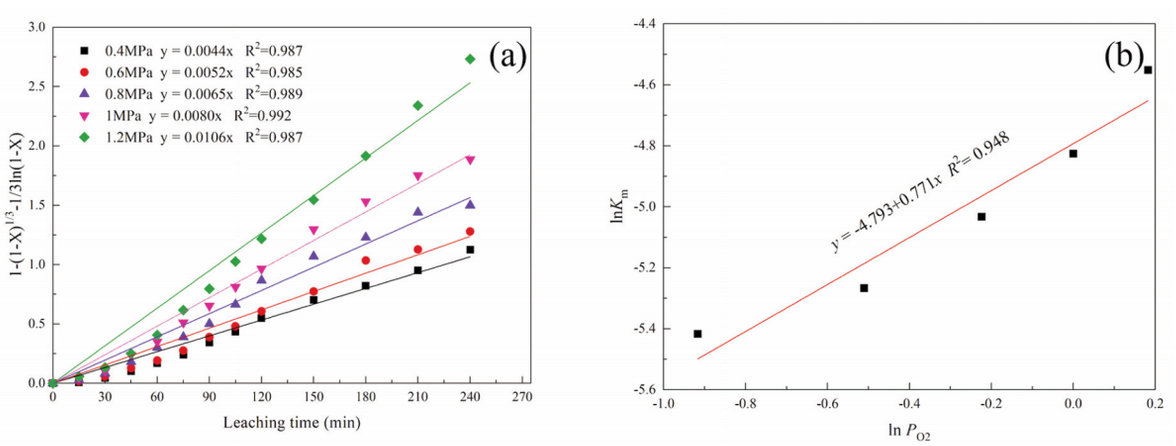

Figure 13. *(a) Fitting results of mixing control models under different oxygen partial pressures and (b) fitting results of lnK and lnP_{O2} at different oxygen partial pressures during leaching*

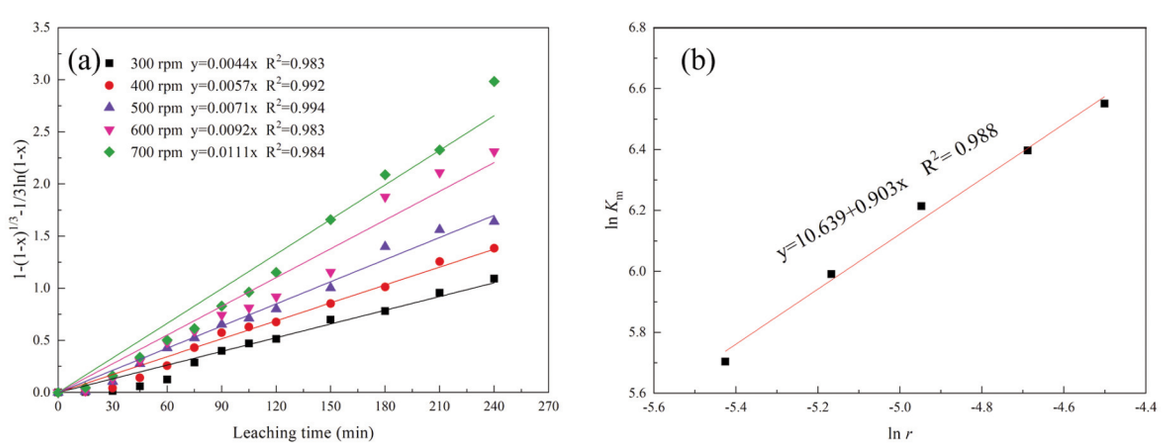

Figure 14. *Fitting results of mixing control model at different stirring speeds (a) and results of ln k and ln r at different stirring speeds during leaching (b)*

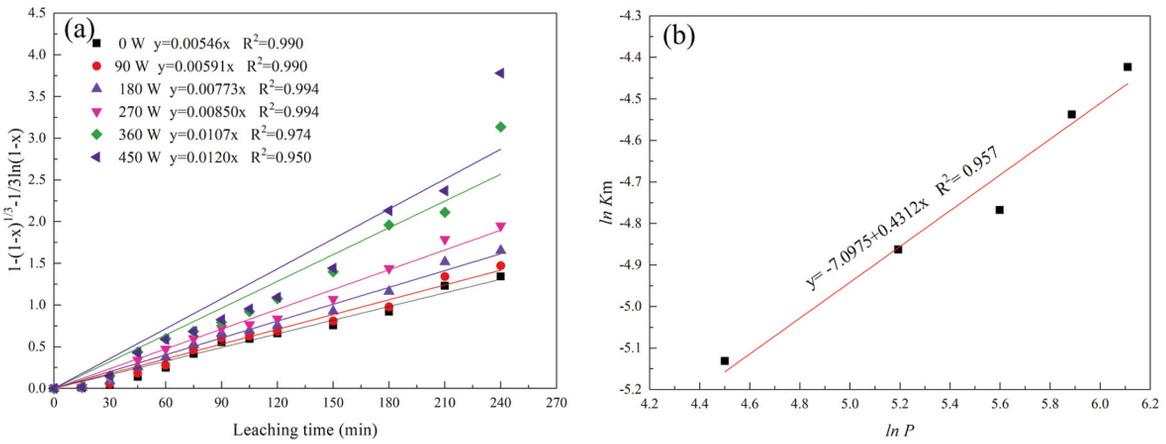

Figure 15. *(a) Fitting results of mixing control under different ultrasonic powers and (b) relationship between lnK_m and lnP in leaching process*

shown in Figure 14(a). The natural logarithm (lnK_m) of constant speed K_m obtained within the range of 300 to 600 r/min was plotted against the natural logarithm (lnr) of stirring speed (see Figure 14(b)), and linear fitting was carried out, resulting in the reaction order (n_2) of stirring speed was obtained as 0.903.

3.3.2.3. Reaction order of ultrasonic power

Leaching data related to ultrasonic power (Figure 9) were brought into the dynamic equation of hybrid control for linear fitting, and the fitting results were shown in Figure 15(a). The natural logarithm (lnK_m) of constant speed K_m obtained from 90 W to 450 W was plotted against the natural logarithm (lnP) of ultrasonic power P, and the linear fitting was carried out. The results were shown in Figure 15(b), and the reaction order (n_3) of ultrasonic power was calculated to be 0.431.

By bringing the corresponding reaction order obtained into the kinetic equation, the macroscopic kinetic equation was expressed as follows:

$$1-(1-X)^{1/3}-1/3ln(1-X)=40.457P_{O_2}^{0.771}r^{0.903}P^{0.431}e^{(-8630.19/T)}t$$

4. Conclusion

1) With water as lixiviate (no acid was added during the leaching process), hydrothermal leaching enhanced with ultrasonic can eco-friendly utilize CPSSC for the selective extraction of copper, and under the conditions of reaction temperature 180 °C, oxygen partial pressure 1.0 MPa, stirring rate of 600 r/min, ultrasonic power of 360 W, liquid to solid ratio of 10:1 and mass ratio of sodium lignosulfonate to raw material of 0.2%, the leaching efficiency of copper from CPSSC reached 99.12%, while the leaching efficiency of iron was only 19.64%.

2) Enrichment with ultrasound caused the efficiency of copper extraction to increase by 10.02% and the leaching efficiency of iron to decrease by 5.20%, demonstrating selective extraction of copper.

3) Kinetics study of the leaching process showed that the leaching process of copper from CPSSC was in line with the unreacted shrinkage core model and belonged to the mixing control. The apparent activation energy of the leaching reaction was 71.76 kJ/mol, and the macroscopic kinetic equation of the leaching reaction could be expressed as:

$$1-(1-X)^{1/3}-1/3ln(1-X)=40.457P_{O_2}^{0.771}r^{0.903}P^{0.431}e^{(-8630.19/T)}t$$

Acknowledgments

The authors express the sincere appreciation to the National Natural Science Foundation of China for the financial support (Project No. 21978122).

Author's contribution

Qingfeng Liu: Investigation, Methodology, Software, Fitting, Formal analysis, Validation, Data curation, Writing–original draft. Yalong Liao: Resources, Supervision, Project administration, Paper modification and editing. Jialei Li: Investigation, Data curation, Formal analysis. Min Wu: Investigation, Data curation.

Data availability

Data availability will be provided by request, and there is none conflict of interest.

Declaration of interest statement

This article has not been published elsewhere in whole or in part. All authors have read and approved the content, and agree to submit for consideration for publication in the journal. There are no any ethical/legal conflicts involved in the article.

References

[1] J.X. Hu, G.C. Tian, F.T. Zi, X.Z. Hu, Leaching of chalcopyrite with hydrogen peroxide in 1-hexyl-3-methyl-imidazolium hydrogen sulfate ionic liquid aqueous solution, Hydrometallurgy, 169 (2017) 1-8. https://doi.org/10.1016/j.hydromet.2016.12.001

[2] R.T. Jones, Electronic structures of the sulfide minerals sphalerite, wurtzite, pyrite, marcasite, and chalcopyrite, (eds) Adelaide: University of South Australia, (2006) 5-80.

[3] H. Nourmohamadi, M.D. Esrafili, V. Aghazadeh, DFT study of ferric ion interaction with passive layer on chalcopyrite surface: Elemental sulfur, defective sulfur and replacement of M^{2+} (M=Cu and Fe) ions, Computational Condensed Matter, 26 (2021) e00536. https://doi.org/ 10.1016/j.cocom.2021.e00536

[4] S.F. Wu, C.R. Yang, W.Q. Qin, F. Jiao, J. Wang, Y.S. Zhang, Sulfur composition on surface of chalcopyrite during its bioleaching at 50 °C, Transactions of Nonferrous Metals Society of China, 25 (12) (2015) 4110-4118. https://doi.org/10.1016/S1003-6326(15)64062-6

[5] G. Mucsi, A review on mechanical activation and mechanical alloying in stirred media mill, Chemical Engineering Research and Design, 148 (2019) 460-474. https://doi.org/10.1016/j.cherd.2019.06.029

[6] S.X. Zhao, G.R. Wang, H.Y. Yang, G.B. Chen, X.M. Qiu, Agglomeration-aggregation and leaching properties of mechanically activated chalcopyrite, Transactions of Nonferrous Metals Society of China, 31 (5) (2021) 1465-1474. https://doi.org/10.1016/S1003-6326(21)65590-5

[7] K. Maryam, B. Rezai, A.A. Abdollahzadeh, B.P. Wilson, M. Molaeinasab, M. Lundström, Investigation into the effect of mechanical activation on the leaching of chalcopyrite in a glycine medium, Hydrometallurgy, 203 (2021) 105492. https://doi.org/10.1016/j.hydromet.2020.105492

[8] X.B. Wan, J.J. Shi, T. Pekka, A. Jokilaakso, Extraction of copper from copper-bearing materials by sulfation roasting with SO_2-O_2 gas, JOM, 72 (10) (2020) 3436-3446. https://doi.org/10.1007/s11837-020-04300-7

[9] S.D. Lin, L. Gao, Y. Yang, J. Chen, S.H. Guo, M. Omran, G. Chen, Dielectric properties and high temperature thermochemical properties of the pyrolusite-pyrite mixture during reduction roasting, Journal of Materials Research and Technology, 9 (6) (2020) 13128-13136. https://doi.org/10.1016/j.jmrt.2020.09.056

[10] Y.L. Bai, W. Wang, K.W. Dong, F. Xie, D.K. Lu, Y.F. Chang, K.X. Jiang, Effect of microwave pretreatment on chalcopyrite dissolution in acid solution, Journal of Materials Research and Technology, 16 (2022) 471-481. https://doi.org/10.1016/j.jmrt.2021.12.014

[11] M.X. Hong, X.T. Huang, X.W. Gan, G.Z. Qiu, J. Wang, The use of pyrite to control redox potential to enhance chalcopyrite bioleaching in the presence of leptospirillum ferriphilum, Minerals Engineering, 172 (2021) 107145. https://doi.org/10.1016/j.mineng.2021.107145

[12] Z.Y. Tian, H.D. Li, Q. Wei, W.Q. Qin, C.R. Yang, Effects of redox potential on chalcopyrite leaching: An overview, Minerals Engineering, 172 (2021) 107135. https://doi.org/10.1016/j.mineng.2021.107135

[13] L. Li, M. Soleymani, A. Ghahreman, New insights on the role of lattice-substituted silver in catalytic oxidation of chalcopyrite, Electrochimica Acta, 369 (2020) 137652. https://doi.org/10.1016/j.electacta.2020.137652

[14] R. Liao, X.X. Wang, B.J. Yang, M.X. Hong, H.B. Zhao, J. Wang, G.Z. Qiu, Catalytic effect of silver-bearing solid waste on chalcopyrite bioleaching: A kinetic study, Journal of Central South University, 27 (5) (2020) 1395-1403. https://doi.org/10.1007/s11771-020-4375-1

[15] K.T. Konadu, R. Sakai, D.M. Mendoza, C. Chuaicham, H. Miki, K. Sasaki, Effect of carbonaceous matter on bioleaching of Cu from chalcopyrite ore, Hydrometallurgy, 195 (2020) 105363. https://doi.org/10.1016/j.hydromet.2020.105363

[16] M. Kartal, F. Xia, D. Ralph, W.D.A. Rickard, F. Renard, W. Li, Enhancing chalcopyrite leaching by tetrachloroethylene-assisted removal of sulphur passivation and the mechanism of jarosite formation, Hydrometallurgy, 191 (2020) 105192. https://doi.org/10.1016/j.hydromet.2019.105192

[17] T. Wen, Y.L. Zhao, Q.H. Xiao, Q.L. Ma, S.C. Kang, H. Q. Li, S.X. Song, Effect of microwave-assisted heating on chalcopyrite leaching of kinetics, interface temperature and surface energy, Results in Physics, 7 (2017) 2594-2600. https://doi.org/10.1016/j.rinp.2017.07.035

[18] T. Wen, Y.L. Zhao, Q.L. Ma, Q.H. Xiao, T.T. Zhang, J. X. Chen, S.X. Song, Microwave improving copper extraction from chalcopyrite through modifying the surface structure, Journal of Materials Research and Technology, 9 (1) (2020) 263-270. https://doi.org/10.1016/j.jmrt.2019.10.054

[19] J. Cháidez, J. Parga, J. Valenzuela, R. Carrillo, I. Almaguer, Leaching chalcopyrite concentrate with oxygen and sulfuric acid using a low-pressure reactor, Metals, 9 (2) (2019) 189. https://doi.org/10.3390/met9020189

[20] J.J. Xi, Y.L. Liao, G.X. Ji, Q.F. Liu, Y. Wu, Mineralogical characteristics and oxygen pressure acid leaching of low-grade polymetallic complex chalcopyrite, Journal of Sustainable Metallurgy, 8 (2022) 1628-1638. https://doi.org/10.1007/s40831-022-00594-w

[21] J.A. Sarasua, L.R. Rubio, E. Aranzabe, J.L.V. Vilela, Energetic study of ultrasonic wettability enhancement, Ultrasonics Sonochemistry, 79 (2021) 105768. https://doi.org/10.1016/j.ultsonch.2021.105768

[22] J.Q. Xue, W.B. Mao, X. Lu, J.X. Li, Y.J. Wang, M. Wu, Dynamics of ultrasound-assisted oxidation leaching of nickel sulfide concentrate, Chinese Journal of Nonferrous Metals, 20 (5) (2010) 1013-1020. https://doi.org/10.19476/j.ysxb.1004.0609.2010.05.031

[23] G.H. Xia, M. Lu, X.L. Su, X.D. Zhao, Iron removal from kaolin using thiourea assisted by ultrasonic wave,

Ultrasonics Sonochemistry, 19 (1) (2012) 38-42. https://doi.org/10.1016/j.ultsonch.2011.05.008

[24] J.Q. Xue, X. Lu, Y.W. Du, W.B. Mao, J.X. Li, Y.J. Wang, Ultrasonic-assisted oxidation leaching of nickel sulfide concentrate, Chinese Journal of Chemical Engineering, 18 (6) (2010) 948-953. https://doi.org/10.1016/S1004-9541(09)60152-X

[25] J.X. Wang, F. Faraji, A. Ghahreman, Effect of ultrasound on the oxidative copper leaching from chalcopyrite in acidic ferric sulfate media, Minerals, 10 (7) (2020) 633. https://doi.org/10.3390/min10070633

[26] H.S. Yoon, C.J. Kim, K.W. Chung, J.Y. Lee, S.M. Shin, S.R. Kim, M.H. Jang, J.H. Kim, S.I. Lee, S.J. Yoo, Ultrasonic-assisted leaching kinetics in aqueous $FeCl_3$ -HCl solution for the recovery of copper by hydrometallurgy from poorly soluble chalcopyrite, Korean Journal of Chemical Engineering, 34 (6) (2017) 1748-1755. https://doi.org/10.1007/s11814-017-0053-x

[27] J. Rooze, E.V. Rebrov, J.C. Schouten, J.T.F. Keurentjes, Dissolved gas and ultrasonic cavitation - A review, Ultrasonics Sonochemistry, 20 (1) (2012) 1-11. https://doi.org/10.1016/j.ultsonch.2012.04.013

[28] Y.M. Wang, A.X. Wu, C.M. Ai, Experiment and mechanism analysis on leaching process of low grade copper sulfide intensified by ultrasonic wave, The Chinese Journal of Nonferrous Metals, 23 (7) (2013) 2019-2025. https://doi.org/10.19476/j.ysxb.1004.0609.2013.07.033

[29] Z. Zhang, X. Liu, D. Li, Y. Lei, T. Gao, B. Wu, J. Zhao, Y. Wang, G. Zhou, H. Yao, Mechanism of ultrasonic impregnation on porosity of activated carbons in non-cavitation and cavitation regimes, Ultrasonics Sonochemistry, 51 (2019) 206–213. https://doi.org/10.1016/j.ultsonch.2018.10.024

[30] A.A. Ádám, M. Szabados, G. Varga, Á. Papp, K. Musza, Z. Kónya, Á. Kukovecz, P. Sipos, I. Pálinkó, Ultrasound-assisted hydrazine reduction method for the preparation of nickel nanoparticles, physicochemical characterization and catalytic application in suzuki-miyaura cross-coupling reaction, Nanomaterials, 10 (2020) 632. https://doi.org/10.3390/nano10040632

[31] Y.L. Yang, Y.F. Shen, J.G. Chen, Y. Wang, Nanocrystalline nickel coating prepared by pulsed electrodeposition combined with ultrasonic agitation, Acta Metallurgica Sinica, 43 (2007) 883–888. https://doi.org/10.1016/j.actamat.2007.05.024

[32] Z.J. Zhang, Analysis on mechanism and influencing factors of ultrasonic assisted extraction, Science and Technology of Food Industry, 31 (4) (2010) 399-401. https://doi.org/10.13386/j.issn1002-0306.2010.04.084

[33] C.F. Dickinson, G.R. Heal, Solid–liquid diffusion controlled rate equations, Thermochimica Acta, 340/341 (1999) 89-103. https://doi.org/10.1016/S0040-6031(99)00256-7

[34] S. Aydogan, Dissolution kinetics of sphalerite with hydrogen peroxide in sulphuric acid medium, Chemical Engineering Journal, 123 (3) (2006) 65-70. https://doi.org/10.1016/j.cej.2006.07.001

[35] H.H. Wang, G.Q. Li, D. Zhao, J.H. Ma, J. Yang, Dephosphorization of high phosphorus oolitic hematite by acid leaching and the leaching kinetics, Hydrometallurgy, 171 (2017) 61-68. https://doi.org/10.1016/j.hydromet.2017.04.015

[36] L. Li, Y. Bian, X. Zhang, Y. Guan, E. Fan, F. Wu, R. Chen, Process for recycling mixed-cathode materials from spent lithium-ion batteries and kinetics of leaching, Waste Management, 71 (2018) 362-371. https://doi.org/10.1016/j.wasman.2017.10.028

[37] W.N. Mu, X.Y. Lu, F.H. Cui, S.H. Luo, Y.C. Zhai, Transformation and leaching kinetics of silicon from low-grade nickel laterite ore by pre-roasting and alkaline leaching process, Transactions of Nonferrous Metals Society of China, 28 (1) (2018) 169–176. https://doi.org/10.1016/S1003-6326(18)64650-3

[38] L. Xiao, P.W. Han, Y.L. Wang, G.Y. Fu, Z. Sun, S.F. Ye, Silver dissolution in a novel leaching system: Reaction kinetics study, International Journal of Minerals Metallurgy and Materials, 26 (2) (2019) 168-177. https://doi.org/10.1007/s12613-019-1721-0

[39] J. Tian, J.Q. Yin, R. Chi, G. Rao, M. Jiang, K. Ouyang, Kinetics on leaching rare earth from the weathered crust elution-deposited rare earth ores with ammonium sulfate solution, Hydrometallurgy, 101 (3/4) (2010) 166-170. https://doi.org/10.1016/j.hydromet.2010.01.001

HIDROTERMALNO PONAŠANJE TOKOM LUŽENJA KOMPLEKSNOG POLIMETALNOG SEKUNDARNOG SULFIDNOG KONCENTRATA POBOLJŠANOG ULTRAZVUČNOM OBRADOM

Q.F. Liu, Y.L. Liao*, J.L. Li, M. Wu

Fakultet za metalurško i energetsko inženjerstvo, Univerzitet za nauku i tehnologiju u Kunmingu, Kunming, Kina

Apstrakt

Složeni polimetalni sekundarni sulfidni koncentrat (CPSSC) teško je efikasno iskoristiti zbog njegove specifične mineralne fazne strukture i visokog sadržaja olova i željeza. U ovoj studiji predložen je novi proces – hidrotermalno luženje bez upotrebe kiseline (voda kao rastvarač), poboljšano ultrazvučnom obradom, kojim se može postići ekološki prihvatljiva i selektivna separacija bakra iz CPSSC-a, uz sprečavanje nastanka opasnog materijala plumboferita u lužnom ostatku. Ispitivan je uticaj kontrolnih parametara na efikasnost luženja, kao i na mineralni fazni sastav i strukturu dobijenog ostatka luženja. Dobijeni rezultati pokazuju da je efikasnost luženja bakra bez sumporne kiseline najveća pod sledećim uslovima: temperatura od 180 °C, parcijalni pritisak kiseonika 1,0 MPa, brzina mešanja 600 °/min, snaga ultrazvuka 360 W, odnos tečnosti i čvrste supstance 10:1 i maseni odnos lignosulfonata i sirovine 0,2%. U optimalnim uslovima, efikasnost luženja bakra i željeza iznosila je 99,12% i 19,46%, respektivno. Pojačanje ultrazvukom povećava efikasnost luženja bakra za 10,02%, dok istovremeno smanjuje efikasnost ispiranja željeza za 5,20%. Proces luženja odgovara modelu nekonvertovanog kontrakcionog jezgra pod mešovitom kontrolom, pri čemu je aktivaciona energija 71,76 kJ/mol, a makroskopska kinetička jednačina u zavisnosti od brzine mešanja, parcijalnog pritiska kiseonika i snage ultrazvuka glasi:
$1-(1-X)^{1/3}-1/3\ln(1-X) = 40.457P_{O_2}^{0.071}r^{0.903}e^{(-8630.19/T)}t.$

Ključne reči: *Halkopirit; Unapređenje procesa; Hidrotermalno luženje; Kinetika*